Three-Dimensional Tomography of Cellulose Nanofibers- Polypeptides Nanocomposite Hydrogels

Tzu-Yi Yu, Yun-Hsiu Tseng, Ming-Chung Wu, Cheng-Si Tsao, and Wei-Fang Su

1 Introduction

In tissue engineering, researchers employ biomaterials to accelerate the rate of self-regeneration of damaged tissues [1–4]. This approach is practical if the biomaterials are similar to the environment supporting the target cells [5]. Extracellular matrix, ECM, is the matter between cells. It balances the chemical environment between cells, supports cell growth, and provides stimuli to guide cell differentiation. Most of the polymeric biomaterials for tissue engineering can hardly mimic both the microstructure and the biochemical environment of ECM. Recently, a type of nanomaterial derived from nature cellulose called "cellulose nanofiber" is an emerging ECM-mimic biomaterials. Cellulose nanofibers, CNFs, are synthesized by applying physical and chemical treatments to nature cellulose, such as woods and pulps [6]. This nanomaterial features its tunable crystallinity and surface chemistry according to the physical and chemical treatments during its synthesis [7–9]. Though many groups reported its excellent biocompatibility and applied CNFs hydrogels in tissue engineering, so far, these CNFs hydrogels crosslinked by cationic ions lack of biochemical stimuli leading to malfunction organoids [10–12]. Here, a new CNFs hydrogel system crosslinked with polypeptides is proposed to demonstrate the possibility of combining a synthetic polypeptide in CNFs hydrogels. In this research, the CNFs hydrogels were crosslinked with two types of crosslinkers—calcium cation (from calcium chloride, $CaCl_2$) and poly L-lysine-*random*-L-glutamic acid (PLLGA). The

T.-Y. Yu · Y.-H. Tseng · W.-F. Su (✉)
Department of Materials Science and Engineering, National Taiwan University, Taipei, Taiwan
e-mail: suwf@ntu.edu.tw

M.-C. Wu
Department of Chemical and Materials Engineering, Chang-Gung University, Taoyuan, Taiwan

C.-S. Tsao
Institute of Nuclear Energy Research, Longtan, Taoyuan, Taiwan

K.-P. Lin et al. (eds.), *Future Trends and Challenges of Molecular Imaging and AI Innovation*, Springer Proceedings in Physics 272,
https://doi.org/10.1007/978-3-030-92786-8_6

effect of crosslinker types on the CNFs hydrogels' microstructure in different scale was studied using four imaging techniques: small angle X-ray scattering (SAXS), scanning electron microscope (SEM), transmission X-ray microscope (TMX), and polarized optical microscope (POM).

2 Materials and Method

A. Nomenclature

CNF stands for "cellulose nanofiber", $PLL_{80}GA_{20}$ (or PLLGA) stands for the random copolymer of L-lysine and glutamic acid in the ratio of 4 to 1. CNF is the main component of hydrogels, and PLLGA is a synthetic polypeptide as one of crosslinkers to CNF hydrogel. The CNF hydrogel crosslinked by PLLGA is named CNF/PLLGA. Similarly, the CNF hydrogel crosslinked by $CaCl_2$ is named CNF/$CaCl_2$. POM is the abbreviation to "polarized optical microscope", and SAXS represents "small angle x-ray scattering".

B. Materials and Hydrogel Fabrication

The calcium chloride was used as purchased. PLLGA was synthesized by the ring-opening polymerization (ROP) and the hydrolysis of protecting groups. The detail of PLLGA synthesis refers to the literature [13]. The numbers of PLLGA repeating units were controlled around 100 ~ 150. The CNFs suspension was synthesized with TEMPO oxidation and $NaBH_4$ reduction. Before fabricating the CNFs hydrogels, the crosslinkers ($CaCl_2$ and PLLGA) were dissolved in DI water to prepare the crosslinker solution in 50 mM effective charge concentration.

The CNFs hydrogels were fabricated with the dropped method reported in the literature about CNFs hydrogels [10, 12, 14]. The crosslinker solution was gently dropped in the container with CNFs suspension to form the CNFs hydrogels. After immersion for one night, the supernatant was removed, and the CNFs hydrogel was immersed in DI water for another night to remove the excessive crosslinker. The CNFs composite hydrogels were prepared with 1 ml of CNFs suspension and 2 ml of crosslinker precursors.

C. Polarized Optical Microscope

The hydrogels were observed under POM (DM 2500 M, LEICA). To prevent the hydrogels from desiccation, they were immersed in DI water before characterization. In this research, the hydrogels were characterized under two modes: "Cross Polar" and "Cross Polar + Compensator". In cross-polar mode, the polarity of analyzer was vertical to of polarizer. While the black region represents amorphous or isotropic crystal phases, the white area represents anisotropic structure from oriented polymer chain or, in this study, nanofibers. By adding a compensator in the light path, the orientation of microstructures was distinguished by their colors. Purple regions were amorphous or isotropic crystals. In blue areas, polymer chains or nanofibers

were oriented from right-up to left-down in images. For those in orange areas, their orientation is from left-up to right-down.

D. Small Angle X-Ray Scattering

The transmission SAXS data of CNFs hydrogels were obtained at 23A work station in National Synchrotron Radiation Research Center, NSRRC. The beam energy was 15 keV, the sample-to-detector distance was 3.875 m, and the q range was from 0.005 Å-1 to 0.35 Å-1. For good SAXS results, hydrogels' desiccation should be prevented, and the hydrogel samples should be characterized in minutes. The 2D SAXS pattern was further converted into 1D integral by software. The background transmission and scattering image were necessary for 1D integration. The SAXS 1D integral can be fitted by the following Eq. (1), which combines Ornstein–Zernike model and wormlike chain model [15–17].

$$I(q) = \frac{l_1}{1 + q^2\xi^2} + p(q) \tag{1}$$

E. Transmission X-Ray Microscope

The transmission X-ray microscope data of CNFs hydrogels were obtained at the 1B work station in National Synchrotron Radiation Research Center, NSRRC, Taiwan. For the X-ray tomography study, the aqueous hydrogel sample was stained with 0.1% w/v ruthenium tetroxide in ddH2O to enhance the hydrogels' contrast. After 3 h of staining, the sample was washed with methanol. Tear off a hydrogel piece with a thickness of about 14 ~ 17 μm to fix on the holder by polyamide tape. 20 μl gold particle solution (400 ~ 500 nm) was added to the hydrogel as the rotation target. The sample was rotated from -75° to 75°. The 3D structure was reconstructed by computer simulation through 151 cross-section images taken per degree by TXM.

3 Results and Discussion

A. Nanometer-scale Structure of CNF Hydrogels

SAXS is a nanostructure characterization method based on the x-ray scatter resulted from the electron density between phases in materials. Since CNF hydrogels comprise two phases, dense cellulose nanofibers and water in interconnected pores, the 2D scatter patterns present the reciprocal structure of CNF hydrogels network. In literature, a fibrous hydrogel network can be fitted with Eq. (1) [17]. The first term in equation represents the structure factor (fibers network structure), and the slope in low q region ($q < 0.01$ Å^{-1}) is related to the hydrogel mesh size (ξ). The smaller mesh size (ξ) results in the slope in low region (b) closer to -2. In Fig. 1a, the slope of CNF/PLLGA is close to the one of pristine CNF, high than -1. However, the CNF hydrogel crosslinked by $CaCl_2$ exhibits a slope close to -2. It indicates that $CaCl_2$ leads to a CNF network with a smaller mesh size (ξ). This structural change is a

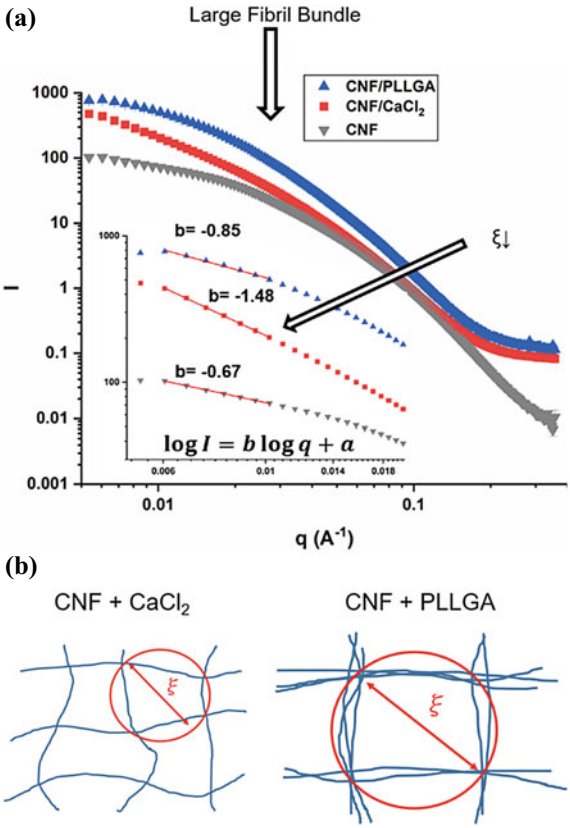

Fig. 1 Microstructure of CNF hydrogel in nanometer scale. **a** SAXS 1D integral of CNFs hydrogels crosslinked by different crosslinker precursors under 50 mM effective charge concentration. The slope at low-q region is related to the mesh size of network,ξ. **b** Simplified illustration of $CNF/CaCl_2$ and CNF/PLLGA. CNF assembles into bundles after adding PLLGA while CNF forms dense network after adding $CaCl_2$

typical result when polymer backbones are crosslinked by adding crosslinkers. On the other hand, the CNF/PLLGA SAXS result suggests a different hydrogel network structure from typical polymeric hydrogels. The second term in Eq. (1) is credited to the morphology of individual CNFs. Because it shows stronger scattering in middle q region, CNF/PLLGA SAXS result leads to a hypothesis that CNFs assembled into bundles when they crosslinked by PLLGA. Two CNF hydrogel networks resulted from either $CaCl_2$ or PLLGA are summarized in Fig. 1b. The network structure difference might lead to different physical properties, such as mechanical strength and water content.

B. Micrometer Scale Structure of CNF Hydrogels

Freeze-dried hydrogel samples are commonly used for structural analysis under scanning electron microscope. The morphologies of dried $CNF/CaCl_2$ and CNF/PLLGA hydrogels are shown in Fig. 2a and b, respectively. In SEM images, the type of crosslinkers has no significant effect on hydrogel structure in network morphologies. However, these images might not present the real network structure due to the distortion of hydrogel structure during sample preparation. To prepare SEM imaging

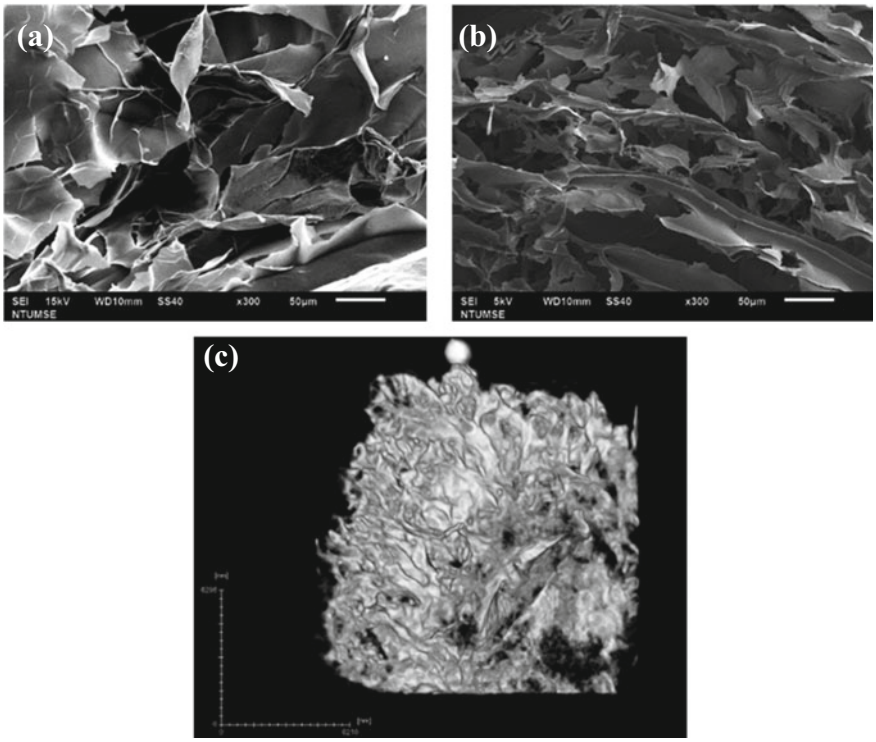

Fig. 2 Interconnected porous structure in CNF hydrogels in the micrometer scale. SEM image of (**a**) CNF/$CaCl_2$ hydrogels and (**b**) CNF/PLLGA. Scale bar represents 50 μm in (**a**) and (**b**). (**c**) Reconstructed 3D model of CNF/$CaCl_2$ hydrogel from Transmission X-ray Microscope. Scale bar represents 6 μm

sample, hydrogel samples have to be frozen and lyophilized to remove water. Ice crystallization brings distortion to its network structure. Scientist still use the pore size in hydrogel SEM image to estimate the hydrogel network density.

Transmission X-ray Microscope (TXM) is an emerging technique to construct hydrogel network images without distortion. In TXM, hydrogel samples are located on a rotatory holder, and the images are collected with different x-ray incident angles. 3D tomography structure of hydrogels can be constructed by compiling these images with a numerical method. In Fig. 2c, the 3D tomography model of CNF/$CaCl_2$ is shown. The hydrogel samples were immersed in a ruthenium tetroxide aqueous solution to enhance contrast. Thus, the region in white represents the interconnected pore filled with water. Comparing with morphology in Fig. 3a, CNF/$CaCl_2$ exhibits high network density and, unlike the flake structure in the SEM image, anomalous CNF domains in TXM. Because hydrogels can be observed by TXM under ambient conditions, the structural distortion during freeze-drying can be prevented. It leads to a realistic image of three-dimensional hydrogel networks in the micrometer scale.

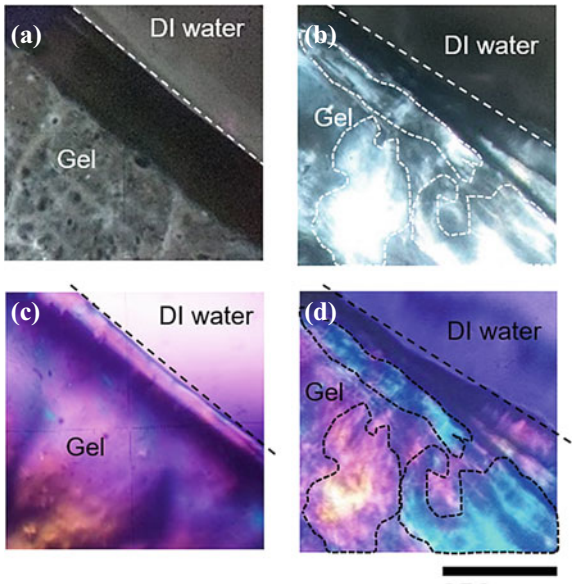

Fig. 3 Birefringence domains in CNF/PLLGA hydrogel induced by PLLGA. Cross-polar image of (**a**) CNF/$CaCl_2$ and (**b**) CNF/PLLGA hydrogel without the compensator. Cross-polar image of (**c**) CNF/$CaCl_2$ and (**d**) CNF/PLLGA hydrogel with compensator. Scale bar represents 250 μm

C. CNF Hydrogels under Polarized Optical Microscope

Most polymeric hydrogels have little optical structure under an optical microscope because they are composed of random coil polymer chains without ordered structures. However, some exhibit birefringence under POM for their order molecular orientation or liquid–crystal-like microstructure [18]. When CNFs are oriented into an ordered structure, CNF hydrogels show such property for the cellulose anisotropic crystal domain within CNF [7, 8, 19]. In Fig. 3b, there are several birefringence regions (white region) in CNF/PLLGA hydrogel, while DI water (background) shows no optical signal. By adding a compensator in the light path, these birefringence regions can be distinguished into two domains in either blue or orange, labeling two orientations. On the other hand, there is no significant birefringence observed in CNF/$CaCl_2$ in Fig. 3a and c. This result supports the previous hypothesis - CNFs assembles into bundles after crosslinked by PLLGA- because CNFs must form ordered structures for birefringence. In contrast, CNFs remain single nanofibers after adding $CaCl_2$, so it shows no birefringence in POM.

4 Conclusions

Four structure characterization methods, SAXS, SEM, TXM, and POM, were used to investigate the crosslinker effect on CNF hydrogel network in different scales. Based on SAXS results, we made a hypothesis that CNFs assemble into bundles after crosslinked by PLLGA. Its birefringence confirmed this hypothesis in POM images.

This microstructural difference might lead to a substantial difference in the physical properties of CNF hydrogels. We also demonstrated using TXM 3D tomography on CNF/$CaCl_2$ hydrogel to construct its in situ network structure without distortion during sample preparation.

Acknowledgements This research was supported financially by the Ministry of Science and Technology (MOST), Taiwan, under Contracts MOST 108–2221–E–002–027–MY3.

Conflict of Interest The authors declare that they have no conflict of interest.

References

1. Shekaran A, Garcia AJ (2011) Biochimica et Biophysica Acta (BBA)-General Subjects 1810(3):350–360
2. Lu H, Hoshiba T, Kawazoe N, Chen G (2011) Biomaterials 32(10):2489–2499
3. Pratt AB, Weber FE, Schmoekel HG, Müller R, Hubbell JA (2004) Biotechnol Bioeng 86(1):27–36
4. Sell S et al (2007) Polym Int 56(11):1349–1360
5. Xu C, Inai R, Kotaki M, Ramakrishna S (2004) Tissue Eng 10(7–8):1160–1168
6. Chirayil CJ, Mathew L, Thomas S (2014) Rev Adv Mater Sci 37(1–2):20–28
7. Shak KPY, Pang YL, Mah SK (2018) Beilstein J Nanotechnol 9:2479–2498
8. Isogai A, Saito T, Fukuzumi H (2011) Nanoscale 3(1):71–85
9. Khatri Z, Mayakrishnan G, Hirata Y, Wei K, Kim I-S (2013) Carbohyd Polym 91(1):434–443
10. Zander NE, Dong H, Steele J, Grant JT (2014) Acs Appl Mater Inter 6(21):18502–18510
11. Yang J, Zhang XM, Ma MG, Xu F (2015) Acs Macro Lett 4(8):829–833
12. Basu A, Lindh J, Alander E, Stromme M, Ferraz N (2017) Carbohyd Polym 174:299–308
13. Blout ER, Idelson M (1958) J Am Chem Soc 80(18):4909–4913
14. Masruchin N, Park B-D, Causin V, Um IC (2015) Cellulose 22(3):1993–2010
15. Geng L et al (2017) Cellulose 24(12):5417–5429
16. Mao Y, Liu K, Zhan C, Geng L, Chu B, Hsiao BS (2017) J Phys Chem B 121(6):1340–1351
17. Schoenmakers DC, Rowan AE, Kouwer PHJ (2018) Nat Commun 9(1):2172
18. Wu ZL et al (2011) Macromolecules 44(9):3542–3547
19. Parker RM et al (2016) ACS Nano 10(9):8443–8449